Titanium Dioxide Nanosheets derived from Indonesian Ilmenite Mineral through Post-Hydrothermal Process

Fauzi, Ahmad
Department of Metallurgical and Materials Engineering, Faculty of Engineering, Universitas Indonesia

Latifa Hanum Lalasari
Metallurgical and Materials Research Center- Indonesia Institute of Science

Sofyan, Nofrijon
Department of Metallurgical and Materials Engineering, Faculty of Engineering, Universitas Indonesia

Ferdiansyah, Alfian
Department of Metallurgical and Materials Engineering, Faculty of Engineering, Universitas Indonesia

他

https://doi.org/10.5109/4794174

出版情報：Evergreen. 9 (2), pp.470-475, 2022-06. 九州大学グリーンテクノロジー研究教育センター
バージョン：
権利関係：

Titanium Dioxide Nanosheets derived from Indonesian Ilmenite Mineral through Post-Hydrothermal Process

Ahmad Fauzi[1*], Latifa Hanum Lalasari[2], Nofrijon Sofyan[1], Alfian Ferdiansyah[1], Donanta Dhaneswara[1], Akhmad Herman Yuwono[1*]

[1]Department of Metallurgical and Materials Engineering, Faculty of Engineering, Universitas Indonesia, Depok, 16424, Indonesia

[2]Metallurgical and Materials Research Center- Indonesia Institute of Science, Puspitek Serpong, South Tangerang, Banten, 15314, Indonesia

*Author to whom correspondence should be addressed:
E-mail: ahmad.fauzi82@ui.ac.id, ahyuwono@eng.ui.ac.id

(Received February 11, 2022; Revised June 20, 2022; accepted June 20, 2022).

Abstract: Titanium dioxide (TiO_2) nanosheets are potential candidate material to be developed for photocatalytic applications. The natural resources of TiO_2 are abundant in the form of the mineral ilmenite ($FeTiO_3$). In this work, TiO_2 nanosheets have been synthesized using ilmenite mineral as the precursor through a post-hydrothermal process with temperature variations of 80,100, 120, and 150^oC for 24 hours. The resulting TiO_2 nanosheets were characterized by x-ray diffraction (XRD), scanning electron microscope (SEM) and ultraviolet visible-diffuse reflectance spectroscopy (UV-DRS). XRD analysis showed that the majority phase of the nanosheets was anatase TiO_2 accompanied by a small amount of sodium-titanate. The SEM study reveals the average thickness of nanosheets derived from post-hydrothermal process was 24.86 nm. XRD test results also showed that the increase in post-hydrothermal temperature from 80 to 150^oC has resulted in an increase in the crystallite size of anatase TiO_2 from 35.14 to 45.59 nm. Such increase in the crystallite size has been found to lead to a decrease in the bandgap energy (E_g) of nanosheets from 2.85 to 2.70 eV. These results support the potential use of the resulting TiO_2 nanosheets as the photocatalytic material under the visible light illumination

Keywords: titanium dioxide nanosheets; ilmenite ($FeTiO_3$); optical properties

1. Introduction

Titanium dioxide (TiO_2) is found naturally in form of ilmenite mineral ($FeTiO_3$) with 30-65% content of TiO_2 and other oxide minerals [1, 2]. However, this abundant ilmenite mineral is not currently optimized for use in various applications. This makes it necessary to process ilmenite further to obtain TiO_2 nanostructures. The structures at the nanometer level are assumed to have more pronounced properties than bulk materials. For several optical applications, nanoparticles[3] or zero-dimensional (0-D) nanostructures still have limitations based on their low optical response to visible light that experience fast electron-hole pair recombination, thereby reducing photocatalytic efficiency [4, 5]. Therefore, the modification of the TiO_2 morphology from zero-dimensional (0-D) to one-dimensional (1-D) structures needs to be carried out to overcome the challenges [6]. One-dimensional (1-D) TiO_2 nanostructures such as nanowires, nanorods, nanotubes, and nanosheets are considered ideal for photocatalytic applications. This is because they have a large surface area that can increase the absorption of photon energy in the visible light range, leading to more intensive interaction with the surrounding medium [7, 8].

The hydrothermal technique was used for the formation of the desired TiO_2 nanosheets because it is easy, inexpensive, and environmentally friendly [9, 10]. Furthermore, it has the bandgap energy (Eg) closer to the TiO_2 bulk value of 3.20 eV, which facilitates the electron excitation under the visible light exposure [11] and enhances its photocatalytic performance

A previous study was carried out using the commercial precursor P25 Degussa nanoparticles to produce TiO_2 nanosheets [12]. However, the bandgap energy of the nanosheets obtained was still significantly large at 3.65eV [13]. which is much higher than 3.20 eV of bulk TiO_2[14, 15] Therefore, the nanosheets were not suitable yet for the visible light photocatalysis application [16]. In addition, the P25 Degussa precursor material used has several obstacles such as the import routes, limited stock, and high price For a country like Indonesia which has

abundant mineral deposits, this motivates efforts to obtain an alternative TiO_2 precursor from the local resource, namely $FeTiO_3$ ilmenite mineral [17]. A hydrometallurgical extraction process has also been carried out using the sulfate pathway as a route to convert the ilmenite into TiO_2 [18-22]. In previous studies [23], the extraction process has converted the ilmenite into filtrate and slag/residue. Meanwhile, this study was carried out systematically using the local Indonesia ilmenite slag as the precursor for the formation of TiO_2 nanosheets. The nanosheets obtained were further subjected to post-hydrothermal treatment with temperature variation. This is to enhance the nanocrystalline and reduce the bandgap energy close to the bulk value of anatase TiO_2 for fulfilling the requirement of the expected photocatalytic processes[24].

2. Experimental

Titanate nanosheet was synthesized by hydrothermal method using local Indonesian mineral ilmenite (slag ilmenite resulting from sulfuric acid leaching process) as a precursor. The 10 grams of ilmenite slag was dispersed into 30 ml of 10 M sodium hydroxide (NaOH) solution. The mixed solution was stirred for one hour to homogenize. Then the solution was transferred to a Teflon-coated autoclave. The autoclave was tightly closed and heated at 150ºC for 24 hours in the oven. After the autoclave was slowly cooled to room temperature, the powder product obtained was washed with distilled water, then spelled with 0.1 M hydrochloric acid (HCl), and finally washed with distilled water until the pH value of the treated nanosheets became neutral and dried at 110ºC for 8 hours. Subsequently, post-hydrothermal treatment with varying temperatures (80, 100, 120, and 150ºC) was given for 24 hours. For the purpose of post-hydrothermal treatment, TiO_2 nanosheets were placed on a buffer in a Teflon-coated autoclave to prevent the sample from being in direct contact with water such as cooking rice.

The resulting TiO_2 nanosheets were characterized using X-ray diffraction (Bruker AXS-2θ diffractometer using Cu K-α radiation of 1.5406 Å, operated at 40 kV, 40 mA). The size of the TiO_2 nanosheet crystallites was estimated using the Scherrer equation [25]

$$L = \frac{0.9\,\lambda}{\beta\,cos\theta} \qquad (1)$$

where L is the mean crystal size, λ is the X-ray wavelength, θ is the Bragg angle, and β is the line widening, based on the full width at half maximum (FWHM) in radians [26]. The optical properties of the TiO_2 nanosheets were analyzed using UV-DRS spectrophotometer (UV-1601, Shimadzu). The bandgap energy (E_g) of TiO_2 nanosheets was estimated by analyzing the absorbance spectrum using Tauc plot method [27]. Further confirmation of the nanosheet structure was carried out by observing using SEM (Leica Oxford Instrument, LEO 420i).

3. Result and Discussions

The increased temperature treatment in the post-hydrothermal process produced a dominant anatase phase followed by a minor sodium titanate phase. The anatase phase was formed when the temperature increased due to dehydration of the nanocrystalline Ti-OH interlayered group, leading to a Ti-O-Ti crystal structure [28]. In the process of forming the sodium titanate phase, the Ti-O-Ti bond formula occurs when hydrothermal treatment was carried out, where there are several bond chains of titanium with oxygen. Similarly, it also occurs in the TiO_2 anatase phase during a chain-breaking process to form a new structural phase with Ti-O-Na, Ti-OH bonds, while Na+ and H+ ions exchange take place when the process rises with HCl [29]. Figure 1 showed the XRD pattern for TiO_2 nanosheets that have passed through the post-hydrothermal treatment with temperature variations of 80, 100, 120, and 150ºC. The results of the XRD analysis showed that an increase in the post-hydrothermal temperature of 150ºC increases the diffraction intensity of TiO_2 anatase (Θ). This was indicated by a diffraction peak of 25.10º with a crystal plane (011). It was also discovered that there was an increase in the diffraction intensity of sodium titanate (▲) at 2 θ , namely, 26.93, 34.03, and 52.01º with crystal planes (130), (140) and (440) according to the COD No. 1529535.

Based on Table 1, the relationship between crystallite size and post-hydrothermal temperature showed an increase in the crystallite size of the anatase phase on post-hydrothermal nanosheets. Furthermore, an increase in the diffraction peak's intensity in the XRD pattern showed that the TiO2 nanocrystal grows more significantly from 35.14 to 45.59 nm. as post-hydrothermal temperature increases from 80 to 150ºC

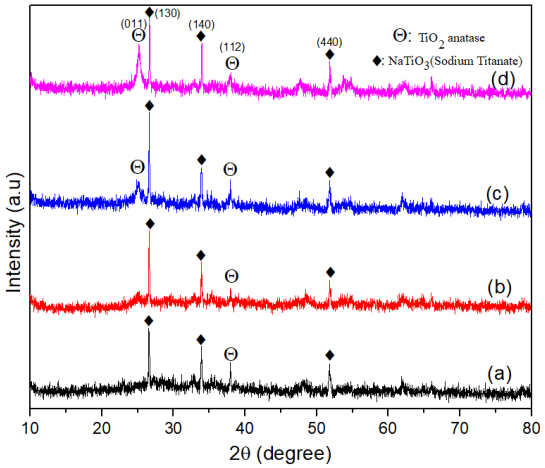

Fig. 1: XRD pattern of TiO_2 nanosheets at various post hydrothermal temperatures: (a) 80, (b) 100, (c) 120, and (d) 150ºC

Table 1. The crystallite size of TiO_2 nanosheet after post-hydrothermal treatment

Code	Post-hydrotermal Temperature (°C)	Crystallite Size (nm)
Sample A	80	35.14
Sample B	100	40.26
Sample C	120	41.00
Sample D	150	45.59

The post-hydrothermal treatment formed the morphological integrity of the TiO_2 nanosheets structure as observed by SEM. The nanosheets structure occurred when TiO_2 crystals were treated with NaOH solution of high concentration, which turned titanate into layers and peels-off to form sheets. Furthermore, the nanosheets has a stable morphology due to the presence of a negatively charged Ti-O- bond and a positively charged Ti-bond on the side of the nanosheets. This makes it impossible for the titanate nanosheets to be rolled up to avoid the formation of nanotubes and maintain the integrity of the nanosheets. The TiO_2 nanosheets has an average thickness of 24.863 ± 0.355 nm and the thickness distribution of the nanosheets with R-Square = 0.88 as shown in Figure 2.

At a temperature of 80°C, the post-hydrothermal treatment showed that some of the nanosheets were not homogeneous and had not formed a perfect TiO_2 nanosheets (Fig.3a). Meanwhile, at 100°C, the morphological structure of titanium dioxide nanosheets looks like sheets that are more homogeneous and clearer (Fig.3b). At 120°C, it was discovered that the titanium dioxide nanosheets have cracked with several piles of powder on top of the nanosheets (Fig.3c). The increase in the temperature of post-hydrothermal treatment to 150°C has been found to be able to maintain the integrity of nanosheet structure and the morphology was homogeneous in a stable condition (Fig,3d).

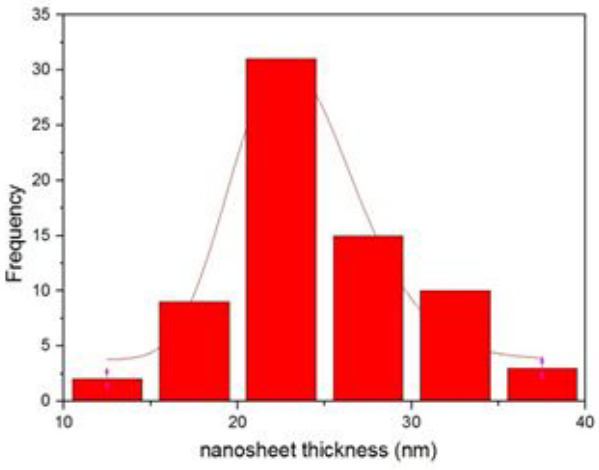

Fig. 2: The thickness distribution of nanosheet TiO_2

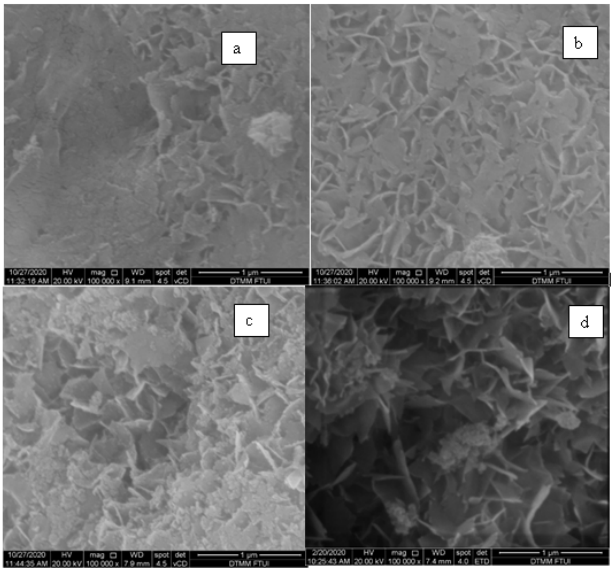

Fig. 3: SEM image of nanosheet TiO_2 at various post hydrothermal temperatures: (a) 80, (b) 100, (c) 120, and (d) 150°C

For determining the relationship between the crystallite size and optical properties of titanium dioxide nanosheets, UV-DRS spectroscopy was carried on the samples. The nanosheet samples show strong absorbance in the ultraviolet region (Fig. 4), while they are relatively transparent in the visible region. In addition, the absorption edges show red-shift from about 550 to 602 nm in wavelength as the post-hydrothermal temperature increased, which can be related to the lower bandgap energy (E_g) of TiO_2 nanosheets as estimated by the using the Tauc plot, which is plotted $(\alpha h\nu)^2$ as a function of photon energy ($h\nu$) given in Fig.5. Based on the results in Fig.5, it can be observed that with increasing post-hydrothermal treatment temperature from 80 to 150°C, the bandgap energy of TiO_2 nanosheets decreased from 2.85 to 2.70 eV.

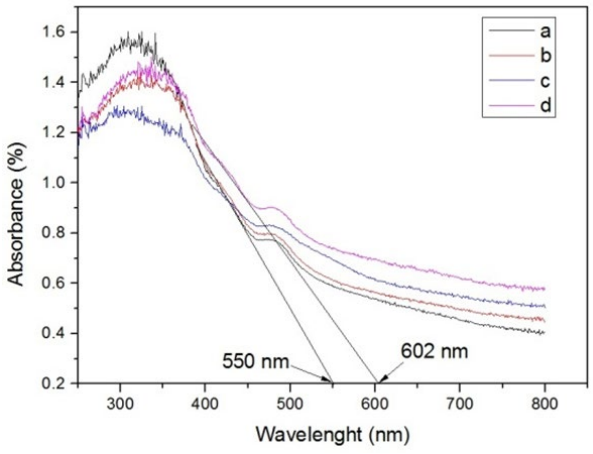

Fig. 4: Absorbance spectra of TiO_2 nanosheet at various post hydrothermal temperatures: (a) 80, (b) 100, (c) 120, and (d) 150°C

The values are rather far below the bulk value of TiO_2 which is 3.20 eV. This can be due to impurities (Fe) in the TiO_2 nanosheet resulted from the nature of ilmenite ($FeTiO_3$). The presence of Fe element can indirectly acts as doping for anatase TiO_2 nanosheets. In addition, the crystallite size of TiO_2 nanosheets also influences the bandgap energy value.This showed that the larger the crystal size, the smaller the bandgap energy [30]. It can be understood that increasing post-hydrothermal temperature in this work is useful for maintaining the structural integrity of TiO_2 nanosheets and facilitating lower bandgap energy so that the resulting nanosheets has the opportunity to be applied as photocatalytic material under the illumination of visible light.

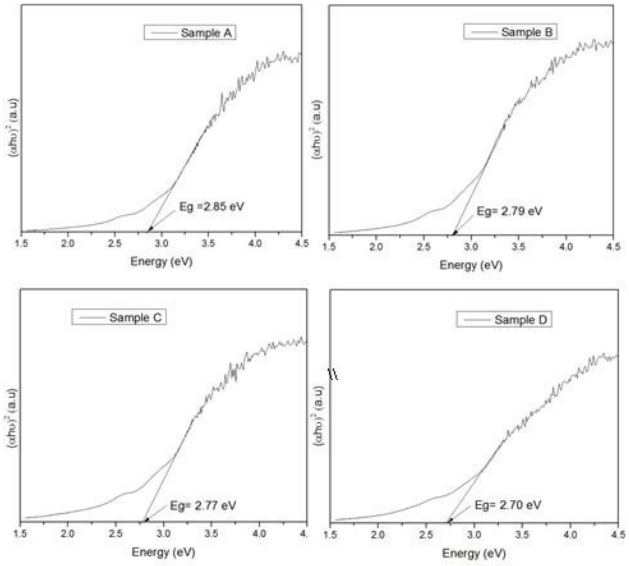

Fig. 5: Band gap energy of TiO_2 nanosheet at various post hydrothermal temperatures: (a) 80, (b) 100, (c) 120, and (d) 150ºC

4. Conclusion

TiO_2 nanosheets have been successfully synthesized from a natural precursor of local Indonesian ilmenite at a low cost through a simple post-hydrothermal process. The XRD study revealed the presence of dominant TiO_2 anatase phase accompanied with small amount of sodium titanate. The post-hydrothermal treatment has succeeded in increasing the crystallite size of the anatase phase significantly from 35.14 to 45.59 nm and managed to maintain the integrity of the TiO_2 nanosheet structure. The increase in the crystallites size of the TiO_2 nanosheet has affected in the decrease in the bandgap energy from 2.85 to 2.70 eV. The resulting bandgap energy is lower than that of the bulk value of TiO_2 anatase which provides opportunities for the material to be used in the photocatalytic applications under visible light illumination.

Acknowledgements

The author is grateful to the Directorate of Research and Development Universitas Indonesia for funding this study through the International Indexed Publication Grant (PUTI Doktor 2020) 2020 based on Agreement/contract number Number: BA-829/UN2.RST / PPM. 00.03.01 / 2020.

References

1) S. Samal, B. Mohapatra, and P. Mukherjee, "The effect of heat treatment on titania slag," *J.Minerals and Materials Characterization and Engineering*., **9** (09)795(2010) .https://www.scirp.org/html/20781.html
2) K.Taira, and H. Einaga, "Distribution Ratio of Pt on Anatase and Rutile TiO_2 Particles, Determined by X-ray Diffraction and Transmission Electron Microscopy Analysis of Pt/TiO_2 (P25)," *Evergreen.*, **5**(4)13-17(2018).doi:https://doi.org/10.5109/2174853.
3) A.C. Opia, M.K.A. Hamid, S. Syahrullail, C.A. Johnson, A.B. Rahim, and M.B. Abdulrahman, "Nano-Particles Additives as a Promising Trend in Tribology: A Review on their Fundamentals and Mechanisms on Friction and Wear Reduction." *Evergreen.,***8**(4)777-798(2021).doi:https://doi.org/10.5109/4742121.
4) D. Chen, Y .Chen, N. Zhou, P. Chen, Y. Wang, K. Li, S. Hou, P. Chwng, P.Peng, R. Zhang, L. Wang, H. Liu, Y. Lu, and R. Ruan, ″Photocatalytic degradation of organic pollutants using TiO_2-based photocatalysts: A review," *J. of Cleaner. Production*., **268** 121725 (2020). doi: https://doi.org/10.1016/j.jclepro.2020.121725.
5) I.H. Dwirekso, and S.M. Ibadurrohman, "Synthesis of TiO_2-SiO_2-CuO Nanocomposite Material and Its Activities for Self-cleaning," *Evergreen*., **7**(02) 285-291(2020).doi:https://doi.org/10.5109/4055234.
6) S. Reghunath , D. Pinheiro, and S.D. KR, "A review of hierarchical nanostructures of TiO_2: Advances and applications," *Applied Surface Science Advances.*, **3** 100063(2021).doi:https://doi.org/10.1016/j.apsadv.2021.100063
7) J. Tian, Z. Zhao, A. Kumar, R.I. Boughton, and H. Liu, "Recent progress in design, synthesis, and applications of one-dimensional TiO_2 nanostructured surface heterostructures: a review," *Chem.Soc.Rev.*, **43**(20) 6920-6937 (2014). doi: 10.1039/C4CS00180J..
8) A. Azani, D.S.C. Halin, M.M.A.F. Abdullah, and K.A. Razak, "The Effect of GO/TiO_2 Thin Film During Photodegradation of Methylene Blue Dye,″ *Evergreen.,***8** (03) 556-564 (2021).doi:https://doi.org/10.5109/4491643.
9) L Lai, E. Lei, C.hu, D.Zhao, W. Zhao, Z.Guo, and D. Huang, "A facile hydrothermal synthesis and properties of TiO_2 nanosheet array films," *Mater. Res.Express*.,**7** (1) 015053 (2020).doi:https://doi.org/10.1088/2053-1591/ab638

b.
10) Z.F. Zahara, “Economic assessment of the sugarcanebased bio-refinery in indonesia,” *Evergreen.*, **5** (2) 67– 77 (2018).
11) N.I.I. Zamri, S.L.N Zulmajdi, E.Kusrini, K. Ayuningtyas, H.M. Yasin, and A. Usman, "Rhodamine B Photocatalytic Degradation using CuO Particles under UV Light Irradiation for Applications in Industrial and Medical Fields." *Evergreen.*, **7** (2) 280-284 (2020). doi: https://doi.org/10.5109/4055233.
12) F. Chen, P. Fang, Y. Gao, Z. Liu, and Y. Dai, "Effective removal of high-chroma crystal violet over TiO_2-based nanosheet by adsorption–photocatalytic degradation," *Chemical Engineering Journal*., **204** 107-113 (2012). doi: https://doi.org/10.1016/j.cej.2012.07.030.
13) L. Sheng, T. Liao, L. Kou, and Z.Sun, "Single-crystalline ultrathin 2D TiO_2 nanosheets: a bridge towards superior photovoltaic devices," *Materials Today Energy*., **3** 32-39 (2017). doi: https://doi.org/10.1016/j.mtener.2016.12.004.
14) C. Kormann, D.W. Bahnemann, and M.R. Hoffmann, "Preparation and characterization of quantum-size titanium dioxide," *J.Phys. Chem*.,. **92**(18) 5196-5201 (1988). doi: https://doi.org/10.1021/j100329a027.
15) M. Ezaki, and K. Kusakabe, "Highly Crystallized Tungsten Trioxide Loaded Titania Composites prepared by Using Ionic Liquids and their Photocatalytic Behaviors," *Evergreen*., (2014). doi: https://doi.org/10.5109/1495159.
16) A.S. Idris, S. Ghosh, and K. Hamamoto, "A multi-layer stacked all sol-gel fabrication technique for vertical coupled waveguide," *Evergreen*., **7**(2) 280-284 (2020). doi:https://doi.org/10.5109/4055233.
17) T.H. Nguyen, and M.S. Lee, "A review on the recovery of titanium dioxide from ilmenite ores by direct leaching technologies," *Mineral Processing and Extractive Metallurgy Review*., **40**(4) 231-247 (2019).doi:https://doi.org/10.1080/08827508.2018.1502668.
18) Y. Liu, T. Qi, J. Chu, Q. Tong, Yi. Zhang, "Decomposition of ilmenite by concentrated KOH solution under atmospheric pressure," *Int. J. Miner. Process*., **81**(2) 79-84 (2006). doi: https://doi.org/10.1016/j.minpro.2006.07.003.
19) L.H. Lalasari, R. Subagja, A.H.Yuwono, F. Firdiyono, S. Harjanto, and B. Suharno, "Sulfuric Acid Leaching of Bangka Indonesia Ilmenite Ore and Ilmenite Decomposed by NaOH," *Advanced Materials Research*., (2013). doi: https://doi.org/10.4028/www.scientific.net/AMR.789.522.
20) L.H. Lalasari, R. Subagja, A.H.Yuwono, F. Firdiyono, S. Harjanto, and B. Suharno, "Preparation, Decomposition and Characterizations of Bangka-Indonesia Ilmenite ($FeTiO_3$) derived by Hydrothermal Method using Concentrated NaOH Solution," *Advanced Materials Research*., (2012). doi:https://doi.org/10.4028/www.scientific.net/AMR.535-537.750.
21) L.H Lalasari, F. Firdiyono, L. Andriyah, A. Suharyanto, T. Arini, A. Ridhova, and N.C. Natasha, "The dissolution of cassiterite Indonesia using hydrometallurgical process in the aerated reactor," *AIP.Conf.Proc*., (2020). doi: https://doi.org/10.1063/5.0002208.
22) A.Fauzi, L.H. Lalasari, N. Sofyan, D. Dhaneswara and A. H. Yuwono, "Synthesis of titanium oxysulfate from ilmenite through hydrothermal, water leaching and sulfuric acid leaching routes," *AIP.Conf.Proc*.,(2020).doi:https://doi.org/10.1063/5.0015864.
23) H.Latifa, A.H. Yuwono, F. Firdiyono, N.T. Rochman, S, Harjanto, B. Suharno, "Controlling the Nanostructural Characteristics of TiO_2 Nanoparticles Derived from Ilmenite Mineral of Bangka Island through Sulfuric Acid Route," *Applied Mechanics and Materials*., (2013). doi: https://doi.org/10.4028/www.scientific.net/amm.391.34.
24) A.H.Yuwono, N. Sofyan, I. Kartini, A.Ferdiansyah. T.H. Pujianto, "Nanocrystallinity enhancement of TiO2 nanotubes by post-hydrothermal treatment," *Advanced Materials Research.*, (2011). doi: https://doi.org/10.4028/www.scientific.net/AMR.277.90.
25) Cullity, B.D, "Elements of X-ray Diffraction," *Addison-Wesley Publishing*., (1956). http://117.239.25.194:7000/jspui/bitstream/123456789/954/1/preliminary%20and%20content.pdf
26) C. Suryanarayana, and M.G. Norton, "X-ray diffraction: a practical approach,".*Springer Science & Business Media*.,1998. https://books.google.co.id/books?hl=id&lr=&id=u7ezrnw3_tgc&o.
27) J. Tauc, R. Grigorovici, and A. Vancu, "Optical properties and electronic structure of amorphous germanium," *phys.stat.sol.,***15**(2) 627-637 (1966).doi:https://doi.org/10.1002/pssb.19660150224.
28) S.Rashad, A. Zaki, and A. Farghali, "Morphological effect of titanate nanostructures on the photocatalytic degradation of crystal violet," *Nanomaterials and Nanotechnology*., **9** 1847980418821778 (2019). doi: https://doi.org/10.1177/1847980418821778.
29) J.Yang, Z. Jin. X. Wang.W. Li, J. Zhang, S. Zhang, X.Guo, and Z. Zhang, "Study on composition, structure and formation process of nanotube $Na_2Ti_2O_4(OH)$," *Dalton.Trans*., 20 3898-3901(2003).doi:https://doi.org/10.1039/B305585J.

30) A.H.Yuwono, B. Liu, J. Xue, J.Wang, H.I. Elim, W. Ji, Y.Li and T.J. White, "Controlling the crystallinity and nonlinear optical properties of transparent TiO_2–PMMA nanohybrids," *J. Mater. Chem*., **14**(20) 2978-2987(2004).doi:https://doi.org/10.1039/b403530e